





Heparin is essential for optimal cell signaling by FGF21 and for regulation of β Klotho cellular stability

Seong J. An^{a,1}, Jyotidarsini Mohanty^a, Francisco Tome^a, Yoshihisa Suzuki^a , Irit Lax^a, and Joseph Schlessinger^{a,1} 

Contributed by Joseph Schlessinger; received November 8, 2022; accepted January 10, 2023; reviewed by Genaro Hernandez and Jorge Moscat

While important insights were gained about how FGF21 and other endocrine fibroblast growth factors (FGFs) bind to Klotho proteins, the exact mechanism of Klotho/FGF receptor assembly that drives receptor dimerization and activation has not been elucidated. The prevailing dogma is that Klotho proteins substitute for the loss of heparan sulfate proteoglycan (HSPG) binding to endocrine FGFs by high-affinity binding of endocrine FGF molecules to Klotho receptors. To explore a potential role of HSPG in FGF21 signaling, we have analyzed the dynamic properties of FGF21-induced FGF21- β Klotho-FGFR1c complexes on the surface of living wild-type (WT) or HSPG-deficient Chinese hamster ovary (CHO) cells by employing quantitative single-molecule fluorescence imaging analyses. Moreover, detailed analyses of FGF21 and FGF1 stimulation of cellular signaling pathways activated in WT or in HSPG-deficient CHO cells are also analyzed and compared. These experiments demonstrate that heparin is required for the formation of FGF21- β Klotho-FGFR1c complexes on the cell membrane and that binding of heparin or HSPG to FGFR1c is essential for optimal FGF21 stimulation of FGFR1c activation, mitogen-activated protein kinase responses, and intracellular Ca^{2+} release. It is also shown that FGF1 binding stimulates assembly of β Klotho and FGFR1c on cell membranes, resulting in endocytosis and degradation of β Klotho. We conclude that heparin or HSPG is essential for FGF21 signaling and for regulation of β Klotho cellular stability by acting as a coligand of FGFR1c.

cell signaling | proteoglycans | endocrine FGFs | phosphorylation

The fibroblast growth factor (FGF) family of cytokines regulate a variety of important cellular processes during embryonic development and in the homeostasis of many adult issues (1–3). The 22 members of the FGF family fall into three categories: canonical FGFs, which signal between cells in a paracrine manner; endocrine FGFs, which act like classical circulating hormones to regulate metabolic pathways in various tissues; and intracellular FGFs, which are not secreted and whose physiological roles in relation to signaling remain unclear (4–6). FGFs mediate their cellular responses by binding to and activating FGF receptors (FGFRs), which belong to a class of the receptor tyrosine kinase (RTK) family of cell surface receptors (7). There are four FGFR genes designated FGFR1, FGFR2, FGFR3, and FGFR4. In general, FGFRs have three immunoglobulin (Ig)-like domains in the extracellular region, designated D1–3. Ig-like domain D3 has particular importance because it is encoded by three exons, which can be alternatively spliced in FGFR1–3, to generate “b” and “c” forms that differ in ligand specificity. While paracrine FGFs can bind to both “b” and “c” forms of FGFR1–3, endocrine FGFs bind only to the “c” form of these receptors and to FGFR4, whose Ig-like domain D3 does not undergo alternative splicing (8).

Compared to other RTK ligands that can bind to and activate their cognate receptors with high affinity, canonical FGFs bind to FGFRs relatively weakly, with dissociation constants in the sub micromolar range (9–11), and consequently depend on a coreceptor—heparan sulfate proteoglycans (HSPGs)—to stabilize FGFR dimerization and induce tyrosine kinase activation (12, 13). In the crystal structure of a ternary FGF-FGFR-heparin complex, heparin is shown to interact not only with FGF to augment FGF-FGFR binding but also with adjoining FGFRs to promote FGFR dimerization (12). Endocrine FGFs, i.e., FGF19, FGF21, and FGF23, on the contrary interact poorly with heparin (14). The weak interaction with heparin is necessary for the endocrine functions of FGF19, FGF21, and FGF23, as it enables them to freely circulate throughout the body, in contrast to canonical FGFs which become trapped by HSPGs that are associated with cells and the extracellular matrix. To compensate for their lack of HSPG binding, endocrine FGFs must bind to different coreceptors to be physically near and activate FGFR. FGF23 requires binding to the coreceptor α Klotho, while FGF19 and FGF21 require binding to the coreceptor β Klotho (15–18). Due to their selective tissue expression, α Klotho and β Klotho furthermore act as “zip code”-like receptors to target signaling by endocrine FGFs (11).

Significance

FGF21 and the two other members of the endocrine FGF family, FGF19 and FGF23, play critical roles in the control of important cellular process. Since a variety of diseases are caused by either enhanced or diminished endocrine FGF activities, FGF21 agonists may provide therapeutic benefits for the treatment of metabolic diseases, while FGF21 antagonists may be beneficial for the treatment of a subtype of liver cancers. Here, we demonstrate that heparin molecules play an essential role in the activation of cellular signaling by FGF21 and for the control of β Klotho cellular stability. These insights into how FGF21 and other endocrine FGF stimulate Klotho-FGFR activation will provide valuable guidance for the development of new FGF21 and other endocrine FGF-based therapeutics.

Author contributions: S.J.A., Y.S., I.L., and J.S. designed research; S.J.A., J.M., F.T., Y.S., and I.L. performed research; S.J.A., J.M., F.T., Y.S., I.L., and J.S. analyzed data; and S.J.A., I.L., and J.S. wrote the paper.

Reviewers: G.H., The University of Texas Southwestern Medical Center; and J.M., Weill Cornell Medicine.

The authors declare no competing interest.

Copyright © 2023 the Author(s). Published by PNAS. This article is distributed under [Creative Commons Attribution-NonCommercial-NoDerivatives License 4.0 \(CC BY-NC-ND\)](https://creativecommons.org/licenses/by-nc-nd/4.0/).

¹To whom correspondence may be addressed. Email: seong.an@yale.edu or joseph.schlessinger@yale.edu.

This article contains supporting information online at <https://www.pnas.org/lookup/suppl/doi:10.1073/pnas.2219128120/-/DCSupplemental>.

Published February 6, 2023.

Because weakened heparin binding is a requisite property of endocrine FGFs, it has long been thought that their signaling does not require HSPG. The current prevailing model is that Klotho proteins substitute for the loss of HSPG binding to endocrine FGFs via Klotho's high affinity and selective binding to endocrine FGF molecules (19). Moreover, direct contacts between Klotho proteins with the extracellular domains of FGFRs enable activation and tyrosine phosphorylation of different tissues in a selective manner (20, 21). FGF21, which is predominantly produced in the liver and acts on adipose tissues and the hypothalamus to regulate energy homeostasis, has received much attention due to its beneficial effects in animal models of metabolic syndrome, such as obesity and diabetes (22–25). FGF21 is also expressed in the exocrine pancreas where it functions in an autocrine fashion as a postprandial secretagog to regulate the release of digestive enzymes (26). Interestingly, the structure of the FGF21– β Klotho complex shows how β Klotho has evolved from glycoside hydrolases, which are sugar-cutting enzymes, to serve as a high-affinity receptor for FGF21 (11). Once FGF21 binds β Klotho, its core FGF domain induces dimerization of FGFR1c to stimulate cell signaling. Mechanistically, it is not clear how FGF21 binding to β Klotho leads to the formation of ternary FGF21–FGFR1c– β Klotho complexes, which is necessary to stimulate the tyrosine kinase activity of FGFR.

In this manuscript, we perform single-molecule fluorescence imaging using total internal reflection fluorescence microscopy (TIRFM) to analyze FGF21-induced signaling complexes on the surface of living cells. By monitoring the lateral mobility and supra-molecular organization of fluorescently labeled β Klotho in cells with and without endogenous HSPG, we demonstrate that heparin is required for the formation of FGF21– β Klotho–FGFR1c complexes. Moreover, heparin is necessary for FGF21 signaling, as ligand-induced activation of mitogen-activated protein kinase (MAPK) and induction of intracellular Ca^{2+} release are negligible in the absence of endogenous HSPG. Providing evidence that β Klotho–FGFR1c heterodimers exist in equilibrium with β Klotho and FGFR1c monomers, we also show that FGF1 not only causes fluorescently labeled β Klotho molecules to become clustered with FGFR1c on cell membranes but also down-regulates β Klotho levels via degradative trafficking. These actions of FGF1 on β Klotho are negated when FGFR1c binding by β Klotho is impaired. Collectively, our findings elucidate the precise mechanism by which ternary FGF21– β Klotho–FGFR1c complexes form on the cell membrane and clarify the role of HSPG in endocrine FGF signaling.

Results

Our goal in this study is to employ biochemical and cellular approaches including single-molecule imaging of fluorescently conjugated β Klotho molecules expressed in the cell membrane of living cells to explore how FGF21 binding to cells harboring FGFR1c together with β Klotho stimulates FGFR1c activation and cell signaling. We also explore a potential role of cellular HSPG and exogenously supplied heparins in FGF21 stimulation of cell signaling. As a population of β Klotho–FGFR1c heterodimeric complexes may exist in the membrane of cells coexpressing these two receptors, we also address the question of whether FGF1, a canonical FGFR ligand, may modulate the function, activity, and dynamic properties of β Klotho in these cells.

Heparin Reduces the Lateral Mobility of Fluorescently Labeled β Klotho Particles in HSPG-Deficient Chinese hamster ovary (CHO) Cells. We previously used single-molecule TIRFM imaging to monitor dimerization of individual α Klotho molecules by FGF23,

which is a bivalent ligand of α Klotho (27). There were several considerations in the design of the present study. First, to make β Klotho fluorescent, we appended HaloTag to the extracellular N terminus of β Klotho so that the cell surface pool of β Klotho could be selectively labeled by a cell-impermeant fluorescent Alexafluor-488 HaloTag ligand. Second, since a low surface density is necessary for single-molecule imaging, we used transient transfection to control the expression level of HaloTag- β Klotho. Third, we used CHO cells due to the availability of a well-characterized line of mutant CHO cells (pgsD-677 cells; ref. 28) that is deficient in HSPG expression. We reasoned it would be necessary to compare wild-type (WT) and HSPG-deficient cells because an effect of exogenous heparin in FGF21 signaling could be made redundant by endogenous HSPG, as previously demonstrated for FGF1 signaling (9). Based on signaling experiments (see below), we confirmed that CHO cells do not express β Klotho but do express a low level of FGFR1, as previously reported (29).

We briefly labeled WT or HSPG-deficient CHO cells transfected with HaloTag- β Klotho with Alexafluor-488 HaloTag ligand for 15 min at 37 °C. Fig. 1A shows a representative TIRFM image of a cell with a very low expression level of HaloTag- β Klotho (*Upper*) and the trajectories of individual HaloTag- β Klotho particles within the same region of the cell (*Lower*). The lateral mobility of particles on the cell surface was quantified by calculating diffusion coefficients from the mean square displacement (MSD) of the trajectories. In both WT and mutant CHO cells, the diffusion coefficients of HaloTag- β Klotho expressed alone (black bars) or with exogenous FGFR1c coexpression (cyan bars) were not significantly different, although they tended to be smaller when exogenous FGFR1c was expressed (Fig. 1B). The addition of FGF21 alone (10 nM, burgundy bar) in WT CHO cells reduced the diffusion coefficient of HaloTag- β Klotho with FGFR1c (by 13.1%, $P < 0.001$), and similar reductions (9.42%, $P < 0.05$ and 14.4%, $P < 0.001$) were seen when heparin (hatched burgundy bars) was included at two different concentrations (4 and 40 $\mu\text{g}/\text{mL}$, respectively). However, in mutant CHO cells lacking HSPG, FGF21 did not reduce the diffusion coefficient of HaloTag- β Klotho by itself and required heparin to do so (by up to 14.1%, $P < 0.001$). Consistent with these data reflecting β Klotho–FGFR1c interactions, FGF21-induced changes in the diffusion coefficient were generally smaller, especially in mutant CHO cells, when exogenous FGFR1c was not coexpressed, i.e., when only a low level of endogenous FGFR1c was present (*SI Appendix, Fig. S1A*).

Changes in the diffusion coefficient were associated with changes in the intensity distribution of HaloTag- β Klotho particles (Fig. 1C). In unstimulated WT and mutant CHO cells coexpressing FGFR1c, the intensity distribution of particles (*Left*) could be fitted with a mixed Gaussian model, consisting of a major peak and a minor peak with nearly twice the intensity (44.4 ± 2.5 vs. 85.2 ± 5.5 a.u., respectively, in mutant CHO cells). The intensity of the major peak corresponds to monomeric HaloTag- β Klotho because it is similar to the intensity of free dye (55.4 ± 1.6 a.u.) absorbed onto glass in our TIRFM setup (27). In WT CHO cells coexpressing FGFR1c, the addition of FGF21 alone or with heparin caused the intensity distribution to become shifted to the right such that the mixed Gaussian fit now contained several peaks. In contrast, in mutant CHO cells lacking HSPG, the addition of FGF21 alone did not substantially alter the intensity distribution, but the inclusion of heparin yielded a mixed Gaussian fit with four peaks that resembled those seen in WT CHO cells.

To determine more conclusively whether FGF21-induced changes in the diffusion coefficient of HaloTag- β Klotho require FGFR1c, we tested L6 cells which do not express endogenous

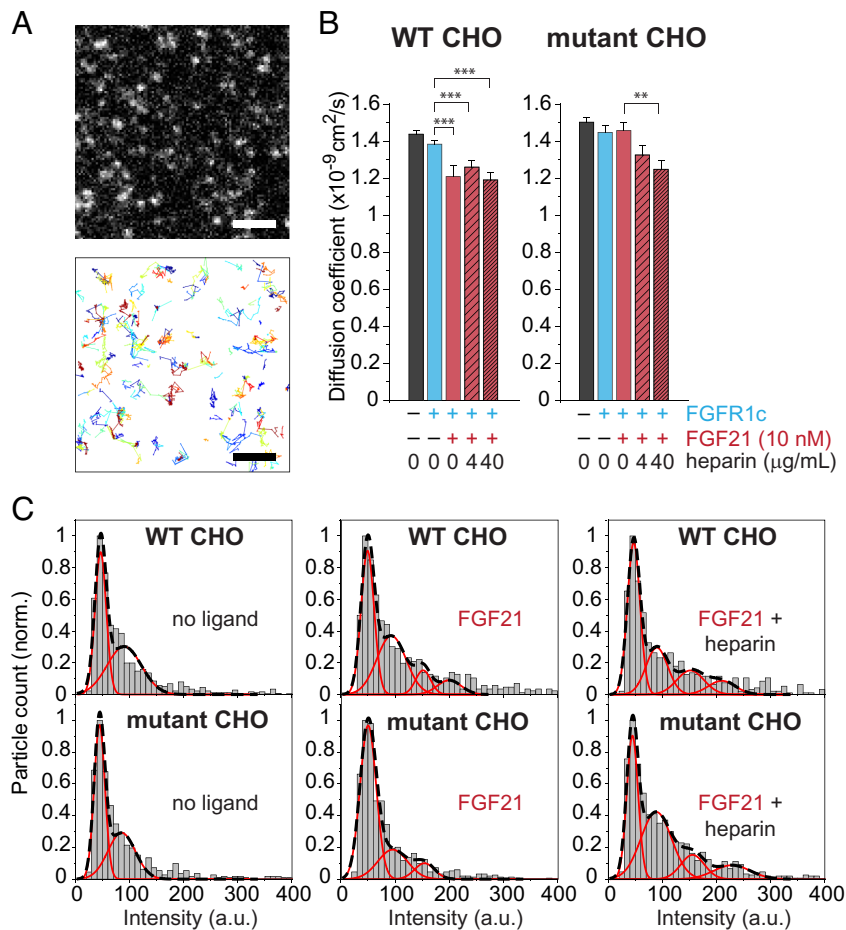


Fig. 1. Single-molecule imaging of HaloTag- β Klotho. (A) Expanded view of HaloTag- β Klotho particles on the surface of a WT CHO cell imaged by TIRFM (Upper). The HaloTag on the extracellular portion of β Klotho was labeled with a cell-impermeant Alexa488 HaloTag ligand. A selected frame (100-ms exposure) from a 10-Hz recording is shown. (Scale bar, 2 μ m.) Automated detection and tracking of moving HaloTag- β Klotho particles during a 10-s recording period (Lower). Single-particle tracking was performed as described in *Materials and Methods*. (B) Diffusion coefficient of HaloTag- β Klotho particles calculated from their MSD in WT and mutant (HSPG deficient) CHO cells under the following conditions: no ligands (40 cells each for WT and mutant cells); FGFR1c only (34 and 41 cells, respectively); FGFR1c and FGF21 (7 and 26 cells, respectively); FGFR1c, FGF21, and 4 μ g/mL heparin (8 and 22 cells, respectively); and FGFR1c, FGF21, and 40 μ g/mL heparin (7 and 23 cells, respectively). Error bars indicate mean \pm SE, ** P < 0.01 and **** P < 0.001 by Student's t test. (C) Representative intensity distributions of HaloTag- β Klotho in cells under the indicated conditions of FGF21 (10 nM) and heparin (40 μ g/mL). Intensities represent the volume under 2D Gaussian fits of the fluorescence of particles. Intensities were taken from the beginning (three frames) of each recording, and their distribution was fitted with a mixed Gaussian model. Black dashed lines, mixed fit. Red lines, individual components.

FGFR1c (30) but do express HSPG. Indeed, FGF21 reduced the diffusion coefficient of HaloTag- β Klotho in L6 cells only when FGFR1c was coexpressed (*SI Appendix, Fig. S2*). As with WT CHO cells, FGF21-induced changes in the diffusion coefficient in L6 cells did not require the addition of heparin. Altogether, these results demonstrate that FGF21 promotes clustering of multiple β Klotho molecules with FGFR1c in a heparin-dependent manner.

FGF21 Signaling in HSPG-Deficient CHO Cells Requires Heparin.

We next examined whether FGF21 signaling requires heparin. For this purpose, we stably transfected WT and HSPG-deficient CHO cells with β Klotho and FGFR1c. The cells were stimulated with increasing concentrations of FGF21 or FGF1, both with and without 5 μ g/mL heparin, for 10 min at 37 $^{\circ}$ C. Lysates were subjected to SDS/PAGE analysis followed by immunoblotting with anti-pFRS2 α antibodies to monitor FRS2 α phosphorylation, anti-pMAPK antibodies to monitor MAPK activation, or anti-MAPK antibodies and anti-FGFR1 antibodies as controls for protein loading. β klotho, which was tagged with a hemagglutinin (HA) peptide, was detected using anti-HA antibodies. In WT CHO cells, the activation patterns induced by FGF1 and

FGF21 were unchanged by the addition of exogenous heparin (*SI Appendix, Fig. S3*): with or without heparin, both FGF1 and FGF21 stimulated tyrosine phosphorylation of FRS2 α and MAPK activation, although tyrosine phosphorylation of FRS2 α by FGF21 was much weaker. In contrast, in mutant CHO cells, the activation patterns induced by FGF1 and FGF21 were different with and without heparin (Fig. 2A). For FGF21-induced stimulation, MAPK activation was robust with heparin, reaching saturation at 10 nM ligand concentration, but virtually absent without heparin. For FGF1-induced stimulation, the heparin dependence was more modest, with MAPK activation reaching saturation at lower ligand concentrations with heparin than without it (0.5 to 1.0 nM vs. 2.5 to 5.0 nM). One explanation for the modest heparin dependence for FGF1 is that, in addition to binding heparan sulfate, FGF1 binds chondroitin sulfate, albeit weakly (31). Since chondroitin sulfate is expressed at elevated levels in mutant CHO cells (28), it may possibly substitute for HSPG in supporting FGF1 signaling in these experiments. Nonetheless, to confirm the well-documented role of HSPG in FGF1 signaling, we also tested FGF1 stimulation in WT and mutant CHO cells stably expressing FGFR1c alone and observed that while MAPK activation is similar in WT CHO cells with or without heparin, it

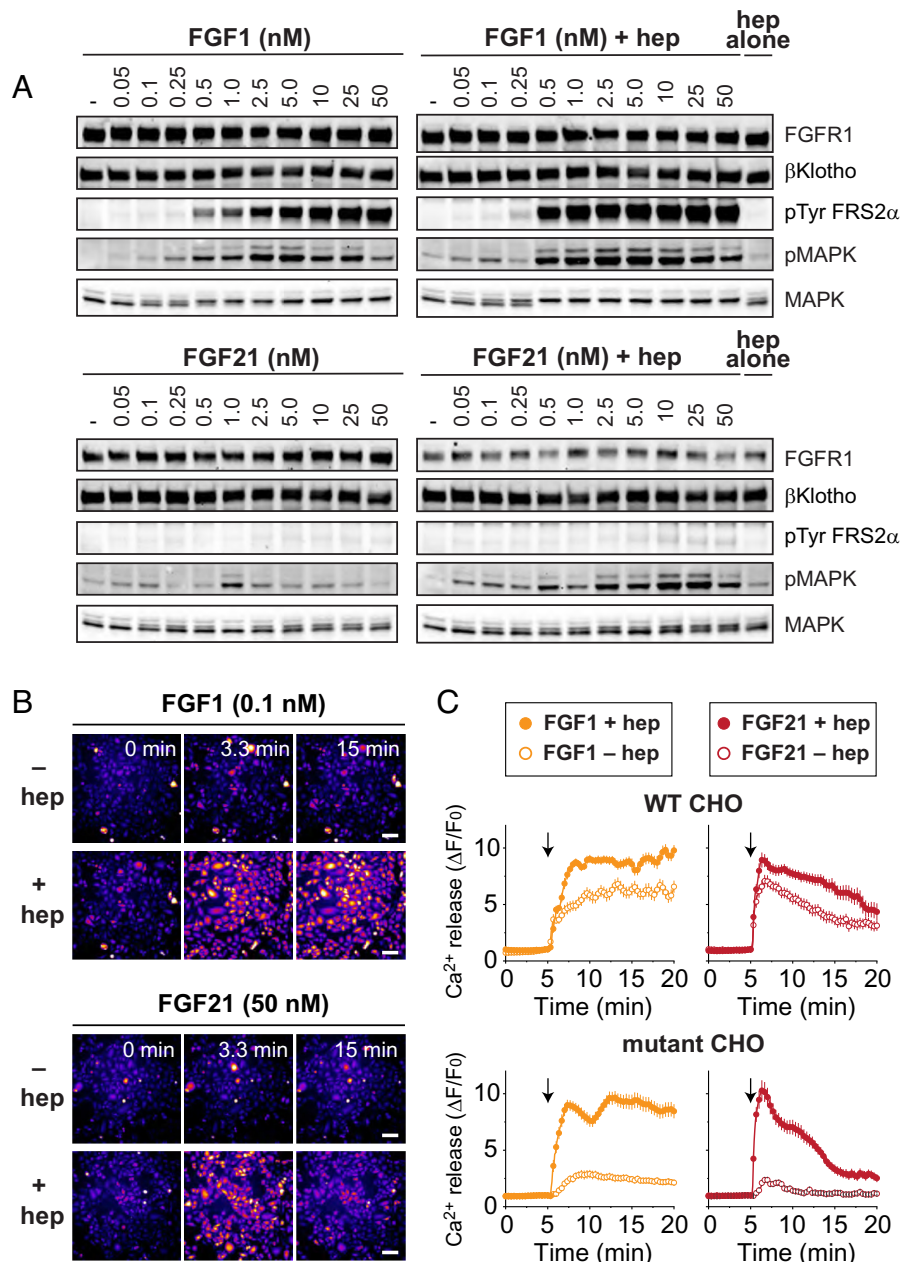


Fig. 2. FGF21-induced stimulation of cell signaling requires heparin. (A) Comparison of the effect of heparin on FGF1 and FGF21-induced tyrosine phosphorylation of FRS2 α and MAPK response. HSPG-deficient CHO cells stably expressing FGFR1c together with β Klotho were left unstimulated or stimulated with either FGF1, FGF1 together with heparin (5 μ g/mL), FGF21, or FGF21 together with heparin (5 μ g/mL) in increasing concentrations (as indicated) for 10 min at 37 $^{\circ}$ C. The cells treated with heparin alone (5 μ g/mL) were used as controls. Cell lysates were subjected to SDS/PAGE and analyzed for tyrosine phosphorylation of FRS2 α and MAPK activation by immunoblotting with anti-pFRS2 α and anti-pMAPK antibodies, respectively. Anti-FGFR1, anti-HA, and anti-MAPK antibodies were used as loading controls. (B and C) Comparison of the effect of heparin on FGF1 and FGF21-induced Ca $^{2+}$ release. WT or HSPG-deficient CHO cells stably expressing FGFR1c together with β Klotho were loaded with the fluorescent Ca $^{2+}$ indicator Calbryte 520 AM and stimulated with either FGF1 (0.1 nM), FGF1 (0.1 nM) together with heparin (40 μ g/mL), FGF21 (50 nM), or FGF21 (50 nM) together with heparin (40 μ g/mL). Fluorescence images of HSPG-deficient CHO cells at the indicated minutes after stimulation (B). Images are displayed using the "Fire" lookup table in ImageJ. (Scale bar, 100 μ m.) Time-course of Ca $^{2+}$ release in WT or mutant (HSPG deficient) CHO cells after the addition (arrow) of the indicated ligands (C). The change in fluorescence (ΔF) was normalized to initial fluorescence (F_0) and plotted as a function of time. Error bars indicate mean \pm SE ($n = 30$ cells for each condition).

is barely induced in HSPG-deficient CHO cells by FGF1 without heparin (SI Appendix, Fig. S4A). Likewise, we confirmed the role of β Klotho in FGF21 signaling by testing FGF21 stimulation in WT CHO cells that stably express FGFR1c alone or FGFR1c together with β Klotho, which showed that β Klotho is required for MAPK activation (SI Appendix, Fig. S5A).

Unlike most signaling pathways (e.g., MAPK) downstream of FGFR activation, Ca $^{2+}$ signaling through activation by phospholipase C γ is mediated directly by FGFR, not through the docking protein FRS2 α (1). Among its metabolic roles, FGF21 induces

intracellular Ca $^{2+}$ release in the exocrine pancreas to release digestive enzymes (26). For these reasons, we also examined the heparin dependence of Ca $^{2+}$ signaling by FGF1 and FGF21, using ligand concentrations that showed strong heparin dependence for MAPK activation. In WT CHO cells stably expressing FGFR1c and β Klotho, both FGF1 (0.1 nM) and FGF21 (50 nM) induced Ca $^{2+}$ release that was only slightly increased by heparin (Fig. 2 B and C). In contrast, in mutant CHO cells, Ca $^{2+}$ release induced by FGF1 and FGF21 was robust only when heparin was added. These results thus demonstrate that heparin is essential for different signaling

pathways activated by FGF21. Notably, Ca^{2+} release was more sustained with FGF1 than with FGF21 stimulation. We observed a similar difference in the duration of MAPK activation by FGF1 and FGF21 (see later).

As with the MAPK activation experiments, we corroborated that Ca^{2+} release by FGF1 requires heparin by also testing WT and HSPG-deficient CHO cells that stably express FGFR1c only (*SI Appendix, Fig. S4B*) and that Ca^{2+} release by FGF21 requires β Klotho by testing WT CHO cells expressing FGFR1c alone or FGFR1c together with β Klotho (*SI Appendix, Fig. S5B*). Finally, in agreement with CHO cells possessing very little endogenous FGFR1 (29), we found that FGF21 with or without heparin failed to induce Ca^{2+} release in parental HSPG-deficient CHO cells and induced only infrequent Ca^{2+} oscillations when β Klotho was stably expressed without exogenous FGFR1c coexpression (*SI Appendix, Fig. S6*).

FGF1 Reduces the Lateral Mobility of β Klotho on the Cell Surface through FGFR1c- β Klotho Interactions. In solution, β Klotho and FGFR1c bind weakly to each other with a dissociation constant (K_d) value of approximately 1 μM (11). In cells, this weak interaction is likely augmented by the reduced dimensionality of the membrane. If β Klotho-FGFR1c heterodimers exist in equilibrium with β Klotho and FGFR1c monomers, then in the process of driving the formation of ternary FGF21- β Klotho-FGFR1c complexes, FGF21 may initially bind to preexisting β Klotho-FGFR1c heterodimers, not just β Klotho monomers. For the same reason, it is possible that FGF1 could indirectly induce clustering of β Klotho as it drives dimerization of FGFR. Thus, to test the idea that β Klotho and FGFR1c interact constitutively, we examined the effect of FGF1 on the lateral mobility of HaloTag- β Klotho, in the same way that we had done for FGF21. In WT CHO cells, the addition of FGF1 alone (orange bar) caused a robust decrease (27.9%, $P < 0.001$) in the diffusion coefficient of HaloTag- β Klotho with FGFR1c compared to the no-ligand condition (cyan bar; Fig. 3A). This decrease was greater than that seen with FGF21 alone in WT CHO cells (Fig. 1A). Interestingly, the inclusion of soluble heparin with FGF1 (hatched orange bars) caused the diffusion coefficient to rise again, resulting in coefficients that fell between those with FGF1 alone and no ligand. This pattern of heparin dependence was not observed in mutant CHO cells because FGF1 did not significantly reduce the diffusion coefficient unless heparin was included. Because i) FGF1 together with heparin produces similar diffusion coefficients in WT and mutant CHO cells, and ii) heparin competes with HSPG for binding to FGF1 and FGFR1c, the smaller effect of FGF1 when heparin is included in WT CHO cells likely reflects the different physical properties of HSPGs and soluble heparin.

To confirm that the above results reflect an interaction between β Klotho and FGFR1c, we deleted a region in β Klotho (residues 544 to 572) that corresponds to the so-called receptor binding arm (RBA) in α Klotho. The RBA was previously shown to mediate α Klotho binding to FGFR1c (21). We imaged HaloTag- β Klotho Δ RBA in mutant CHO cells without ligand or with FGF1 and FGF21. Both ligands were added at 10 nM and with heparin at the higher concentration (40 $\mu\text{g}/\text{mL}$). As shown in Fig. 3B, the diffusion coefficient of HaloTag- β Klotho Δ RBA in cells with FGFR1c was unchanged by the addition of ligands and heparin, indicating an importance for the RBA in the lateral mobility of β Klotho. To validate that β Klotho Δ RBA does not bind FGFR1c, we stably transfected L6 cells with β Klotho WT or β Klotho Δ RBA, both fused to an HA tag, and FGFR1c. The cells were left unstimulated or stimulated with FGF1 (10 nM) or FGF21 (10

nM) with heparin (5 $\mu\text{g}/\text{mL}$) for 10 min at 37 °C. Cell lysates were immunoprecipitated with anti-HA antibodies and subjected to SDS/PAGE and immunoblotting with anti-FGFR antibodies and anti-HA antibodies, to test for β Klotho binding to FGFR1c. The lysates were also analyzed for MAPK activation, MAPK phosphorylation of the receptor, and tyrosine phosphorylation of FRS2 α by immunoblotting with antibodies for pMAPK, pSer-FGFR1, and pFRS2 α , respectively. Anti-FGFR1 and anti-MAPK antibodies were used as loading controls. The results show that β Klotho WT, but not β Klotho Δ RBA, binds FGFR1c (Fig. 3C) and mediates FGF21 signaling (Fig. 3D). FGF1, which does not require β Klotho for signaling, robustly stimulated FGFR activation and MAPK response in cells expressing either β Klotho WT or β Klotho Δ RBA. These experiments thus demonstrate that β Klotho binding to FGFR1c is necessary for ligand-induced changes in the diffusion coefficient of HaloTag- β Klotho.

Consistent with indirect clustering of β Klotho by FGF1, the intensity distribution of HaloTag- β Klotho particles in CHO cells coexpressing FGFR1c could be fitted with mixed Gaussian models containing several peaks when FGF1 was added (Fig. 3E). In WT CHO cells, this redistribution of intensity did not require the addition of soluble heparin. However, in mutant CHO cells lacking HSPG, FGF1 required heparin to produce a similarly large change in the intensity distribution of HaloTag- β Klotho particles. Altogether, these results demonstrate that a monomer-heterodimer equilibrium of β Klotho and FGFR1c molecules allows β Klotho to become clustered with FGFR1c during FGF1-induced receptor dimerization.

FGF1 Promotes Degradative Trafficking of β Klotho. Clustering of β Klotho by FGF1 raises the possibility that β Klotho could be down-regulated by FGF1-stimulated endocytosis and subsequent degradation of FGFR1c. To test this, L6 cells stably expressing FGFR1c and β Klotho fused to an HA tag were left unstimulated or stimulated with either FGF1 (10 nM) together with heparin (5 $\mu\text{g}/\text{mL}$) or FGF21 (10 nM) for various time points at 37 °C. Cell lysates were subjected to SDS/PAGE and analyzed for tyrosine phosphorylation of FRS2 α , MAPK activation, and serine phosphorylation of FGFR1c (by activated MAPK), by immunoblotting with antibodies for pFRS2 α , pMAPK, and pSer-FGFR, respectively. FGFR1c tyrosine phosphorylation was analyzed by immunoprecipitation with anti-FGFR1 antibodies followed by SDS/PAGE and immunoblotting with anti-pTyr. To analyze the level of FGFR1c and β Klotho expression, cell lysates were subjected to immunoblotting with anti-FGFR1 antibodies or immunoprecipitation with anti-HA antibodies followed by immunoblotting with anti- β Klotho antibodies. The data presented in Fig. 4A demonstrate that, in response to FGF1, FGFR1c and β Klotho are both down-regulated within 1 to 3 h. In contrast, in cells stimulated with FGF21, the levels of FGFR1c and β Klotho were unchanged for the duration of the experiment. With respect to signaling, FGF1 induced much greater activation of FGFR1c and its downstream effectors than FGF21 (Fig. 4A). These results suggest that downregulation of FGFR1c and β Klotho levels depends on the strength of FGFR1c activation.

Because protein levels reflect not only the degradation of protein but also its synthesis, we performed cycloheximide chase experiments to monitor β Klotho levels in the absence of de novo protein synthesis. L6 cells stably expressing FGFR1c together with β Klotho fused to an HA tag were treated overnight with cycloheximide (50 $\mu\text{g}/\text{mL}$). The treated cells were left unstimulated or stimulated with either FGF1 (10 nM) together with heparin (5 $\mu\text{g}/\text{mL}$) or FGF21 (10 nM) for various time points at 37 °C. The cell lysates were subjected to SDS/PAGE and analyzed for FGFR1c and

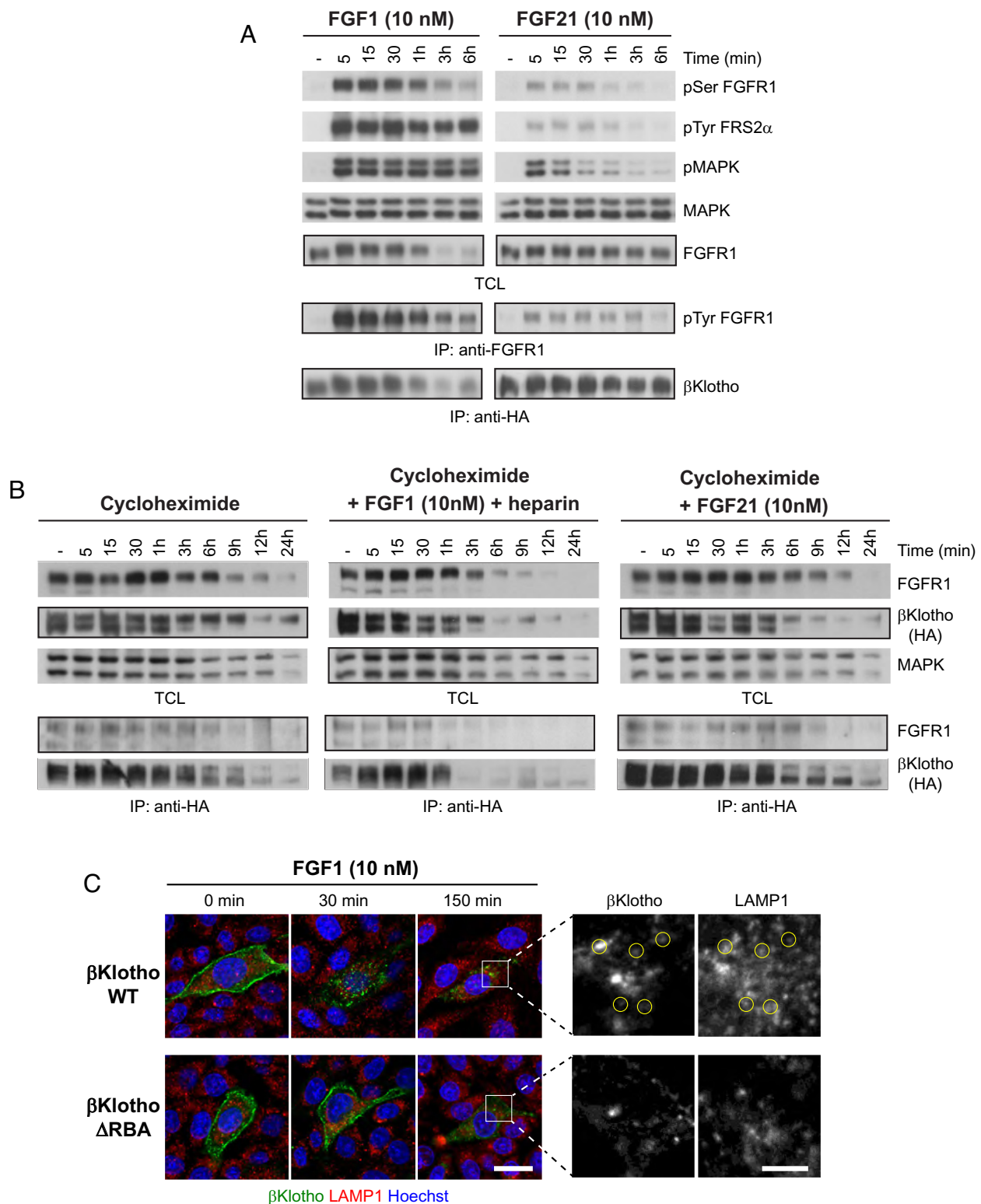


Fig. 4. FGF1 promotes degradative trafficking of βKlotho. (A) L6 cells stably expressing FGFR1c together with βKlotho were left unstimulated or stimulated with either FGF1 (10 nM) together with heparin (5 μg/mL) or FGF21 (10 nM) for the indicated time points at 37 °C. Cell lysates were subjected to SDS/PAGE and analyzed for tyrosine phosphorylation of FRS2α, MAPK activation, and serine phosphorylation of FGFR1c by activated MAPK, by immunoblotting with antibodies for pFRS2α, pMAPK, and pSer-FGFR, respectively. Anti-MAPK antibodies were used as loading control. FGFR1c expression was examined with anti-FGFR1 antibodies. FGFR1c tyrosine phosphorylation was examined by subjecting cell lysates to immunoprecipitation (IP) with anti-FGFR1 antibodies followed by immunoblotting with anti-pTyr antibodies. βKlotho expression levels were determined by subjecting cell lysates to immunoprecipitation with anti-HA antibodies followed by immunoblotting with anti-βKlotho antibodies. TCL, total cell lysate. (B) L6 cells stably expressing FGFR1c together with βKlotho were treated overnight with 50 μg/mL cycloheximide. Treated cells were left unstimulated or stimulated with either FGF1 (10 nM) together with heparin (5 μg/mL) or FGF21 (10 nM) for the indicated time points at 37 °C. Cell lysates were subjected to SDS/PAGE and analyzed for FGFR1c and βKlotho expression using anti-FGFR1 and anti-HA antibodies, respectively. Anti-MAPK antibodies were used as loading control. FGFR1c binding to βKlotho was examined by subjecting cell lysates to immunoprecipitation with anti-HA antibodies followed by immunoblotting with anti-FGFR1c and anti-HA antibodies. (C) CHO cells stably expressing FGFR1c were transfected with HaloTag-βKlotho WT or HaloTag-βKlotho ΔRBA and labeled with Alexafluor-488 HaloTag ligand for 15 min at 37 °C before stimulation with FGF1 (10 nM) together with heparin (40 μg/mL) at 37 °C. The cells were fixed, labeled with Hoechst 33342 to visualize nuclei, and immunostained with LAMP1 antibodies to visualize lysosomes. (Scale bar, 25 μm.)

down-regulate FGFR1c but not β Klotho Δ RBA (SI Appendix, Fig. S7), further supporting that β Klotho and FGFR1c interact with each other on the cell membrane.

Finally, to test whether downregulation of β Klotho by FGF1 is due to degradative trafficking, we examined the subcellular localization of HaloTag- β Klotho during FGF1 stimulation by confocal microscopy. CHO cells stably expressing FGFR1c were transiently transfected with HaloTag- β Klotho or, as a negative control, HaloTag- β Klotho Δ RBA and labeled with Alexafluor-488 HaloTag ligand for 15 min at 37 °C. As in the single-molecule imaging experiments, this protocol labels the cell surface pool of HaloTag- β Klotho. The labeled cells were then stimulated with FGF1 (10 nM) together with heparin (40 μ g/mL) at 37 °C, fixed at various time points, and immunostained with LAMP1 antibodies to visualize lysosomes. Fig. 4C shows that HaloTag- β Klotho, which initially decorates the plasma membrane, is rapidly internalized and appears as numerous intracellular spots within 30 min of stimulation. After an additional 120 min, HaloTag- β Klotho spots can be seen to colocalize with LAMP1 (yellow circles, zoomed region), indicative of degradative trafficking. In contrast, consistent with the lack of downregulation of β Klotho Δ RBA by FGF1 (SI Appendix, Fig. S7), HaloTag- β Klotho Δ RBA internalized much more slowly, remaining on the plasma membrane after 30 min and not showing colocalization with LAMP1 after an additional 120 min.

Discussion

In canonical FGF signaling, the relatively weak affinity between ligand and receptor is compensated by the utilization of HSPGs which function as both coreceptors of FGF and coligands of FGFR molecules. Because HSPGs are ubiquitously present on cell membranes and the extracellular matrix, FGFs cannot diffuse freely upon secretion, which naturally confers an aspect of spatial regulation to their signaling. Indeed, this limited diffusive property is important for canonical FGFs to regulate the highly orchestrated process of tissue development (32, 33). Ironically, some FGFs require the opposite diffusive property so that they can travel between distant tissues to regulate metabolic signaling. In order to circulate, endocrine FGFs have lost their affinity for HSPGs and gained the ability to bind tightly to α Klotho or β Klotho, which are selectively expressed by their target tissues, to activate FGFR. The use of different coreceptors—HSPGs or Klotho proteins—by FGFs has thus led to the long-held idea that a dichotomy exists between canonical and endocrine FGF signaling with respect to heparin dependence. However, what has been less clear is how endocrine FGF signaling could be completely independent of heparin when heparin binding by FGFRs is an essential component of FGF signaling. It is also not clear how FGF19, FGF21, and FGF23 stimulate dimerization and activation of Klotho-FGFR complexes and whether heparin plays a role in endocrine FGF stimulation of cell signaling.

In this report, we show that heparin is in fact essential for FGF21 signaling. Experiments are presented demonstrating that heparin or HSPG function as coligands of FGFRs in FGF21 signaling. As previously demonstrated, β Klotho functions as a coreceptor of FGF21 or more precisely as the high-affinity surface FGF21 receptor. We used single-molecule TIRFM of fluorescently labeled HaloTag- β Klotho in WT and HSPG-deficient cells to demonstrate that multimerization (i.e., activation) of ternary FGF21- β Klotho-FGFR1c complexes on the cell surface requires heparin. Likewise, we demonstrate in signaling experiments with WT and HSPG-deficient cells that FGF21-stimulated activation of MAPK and induction of intracellular Ca^{2+} release depend on

heparin. FGFR1c binds heparin with submicromolar affinity (63 to 450 nM; ref. 34), while FGF21 binding to heparin is too weak to be reliably determined (35). Thus, our data emphasize the importance of heparin binding to FGFR and agree with the role of heparin in promoting receptor dimerization through direct interactions with adjoining FGFRs (12). This conclusion is consistent with experiments demonstrating that in BaF3 cells deficient in HSPG expression, heparin binding to both FGF23 and FGFR1c is necessary for FGF23 signaling (21).

However, receptor dimerization is also mediated by the bivalent binding of FGF to two FGFR molecules (12). In this regard, it is notable that the FGF core of FGF21 binds so weakly to FGFR1c that a precise dissociation constant cannot be determined ($K_d > 10$ to 100 μ M; ref. 11). Our study suggests that FGF21 signaling compensates for this by relying on the interaction between β Klotho and FGFR1c. In solution, these two proteins bind each other with a dissociation constant of ~ 1 μ M (11). The physiological relevance of this interaction has heretofore been unclear. We now show that β Klotho binding to FGFR1c is necessary to form activated ternary FGF21- β Klotho-FGFR1c complexes on the cell surface and to induce signaling by FGF21. This implies that FGF21 is unable to effectively recruit FGFR1c after binding to β Klotho and must bind to β Klotho-FGFR1c heterodimers to promote the formation of ternary FGF21- β Klotho-FGFR1c complexes. Since FGF21 binds tightly to β Klotho ($K_d \sim 20$ to 40 nM; refs. 11 and 36), the properties of FGF21 signaling are largely fine-tuned by the relatively weaker interactions between β Klotho and FGFR1c, the FGF core of FGF21 and FGFR1c, and heparin and FGFR1c. Thus, FGF21-induced FGFR1c activation can be viewed as a coincidence detection event with FGFR1c at the center of three weak binary interactions. The intrinsic instability of this tetrapartite system may explain the generally weaker, more transient signaling induced by FGF21 compared to FGF1, which in turn is likely related to the absence of mitogenic activity with FGF21 signaling (37).

A consequence of the reliance on β Klotho-FGFR1c interactions by FGF21 to stimulate the assembly of signaling complexes is that FGF1 and presumably other canonical FGFs (e.g., FGF2, FGF4, FGF5, FGF6) that activate FGFR1c can down-regulate β Klotho through ligand-induced receptor endocytosis. This is also likely the case for α Klotho, which binds to FGFR1c with high affinity ($K_d \sim 70$ nM; ref. 20). Thus, endocrine FGF signaling in general may be subject to negative regulation by canonical FGF signaling. With respect to FGF21, one scenario in which such crosstalk could occur is in adipose tissues, where FGF21 and FGF1 are both expressed under different nutritional states and known to have pleiotropic effects, including on insulin sensitivity and adipogenesis (38–40). Interestingly, in obese animals, FGF1 expression is up-regulated in white adipose tissue (39, 40) while β Klotho is down-regulated (41–43). The mechanism underlying this β Klotho downregulation is presently unknown. And because obesity-related impairment of FGF21 signaling in this tissue (41, 42) perplexingly persists in adipose-specific β Klotho transgenic mice (43), the physiological ramifications of β Klotho downregulation remain unclear. Thus, in light of our findings, it may be worthwhile to examine the potential interplay between FGF1 and FGF21 signaling in white adipose tissue under normal and obesogenic conditions.

Our proposed mechanism of formation of activated FGF21 and FGF1 signaling complexes in cells that express β Klotho is summarized in Fig. 5. It shows that endocrine FGF signaling not only shares a dependence on HSPGs with canonical FGF signaling, which is necessary for receptor dimerization, but also may be regulated by canonical FGFs through downregulation of β Klotho by

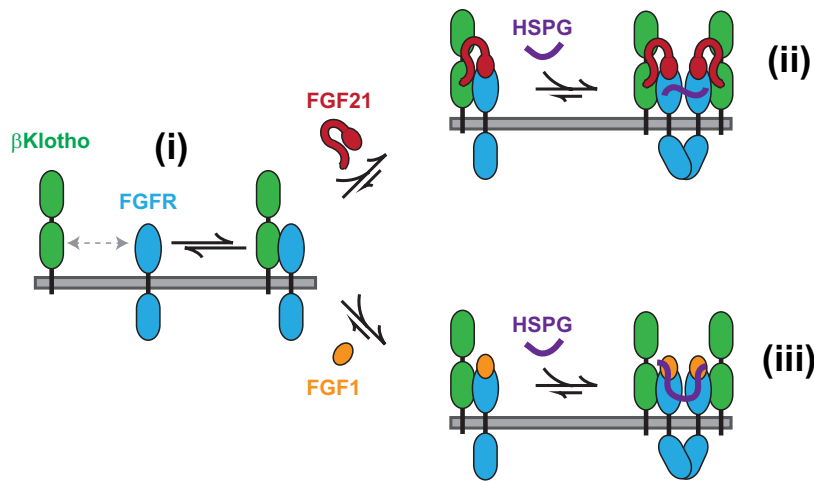


Fig. 5. Mechanism of FGF21 and FGF1 signaling in cells with β Klotho. β Klotho-FGFR1c heterodimers in equilibrium with β Klotho and FGFR1c monomers (i) mediate the formation of FGF21- β Klotho-FGFR1c ternary complexes which are activated by HSPG-dependent dimerization of FGFR1c, with HSPG serving as a coligand for FGFR1c (ii). The same β Klotho-FGFR1c heterodimers cause β Klotho to join FGF1-FGFR1c complexes in canonical FGF1 signaling, resulting in the downregulation of β Klotho by HSPG-dependent dimerization and activation of FGFR1c, with HSPG serving as both a coreceptor for FGF1 and coligand for FGFR1c (iii). For clarity, only the heparan sulfate chain of HSPGs is depicted.

ligand-induced receptor endocytosis, due to interactions between β Klotho and FGFR1c that are essential for FGF21 signaling.

Materials and Methods

Plasmids, Antibodies, Growth Factors, and Reagents. The retroviral vector for C-terminal HA-tagged β Klotho was previously described (11) and made by subcloning full-length β Klotho together with the HA-tag sequence into pBABE-hygro. The viral vector for FGFR1c was previously described (44) and made by subcloning FGFR1c into pBABE-puro. The mammalian expression vector for HaloTag- β Klotho was generated by subcloning β Klotho into a pCMV-N-HaloTag plasmid. The Δ RBA mutant of β Klotho, in which the FGFR1c binding site was deleted (aa Q544-R572), was generated by assembly PCR, followed by standard PCR cloning. pMAPK, MAPK, and HA-tag antibodies were purchased from Cell Signaling Technology. pTyr-FRS2 α and human β Klotho antibodies were purchased from R&D Systems. FGFR1 and pSer-FGFR1 antibodies were generated against the C-terminal tail of FGFR1 (last 18 amino acids) and pSer-779 of FGFR1, respectively. Expression and purification of FGF1 and FGF21 were previously described (refs. 9 and 11, respectively). Heparin (sodium salt from porcine intestinal mucosa) was purchased from Sigma-Aldrich. Cycloheximide (used at a concentration of 50 μ g/mL) was purchased from MilliporeSigma.

Cell Culture. WT CHO cells (CHO-K1) and HSPG-deficient CHO cells (pgsD-677) were obtained from ATCC. CHO cells were cultured at 37 $^{\circ}$ C and 5% CO₂ in F-12K medium (ATCC) supplemented with 10% FBS (Gibco) and 1% penicillin-streptomycin (Gibco). CHO cells stably expressing FGFR1c and β Klotho were generated using the retroviral pBABE vector system and maintained in media with puromycin (10 μ g/mL) and hygromycin B (400 μ g/mL) for FGFR1c and β Klotho selection, respectively. L6 rat myoblasts were obtained from ATCC and cultured at 37 $^{\circ}$ C and 5% CO₂ in Dulbecco's modified eagle medium (DMEM; Gibco) supplemented with 10% fetal bovine serum (FBS; Gibco) and 1% penicillin-streptomycin (Gibco). L6 cells stably expressing FGFR1c together with β Klotho WT or Δ RBA were generated in a similar manner using the retroviral pBABE vector system and maintained in media with puromycin (1 μ g/mL) and hygromycin B (100 μ g/mL).

Immunoprecipitation and Immunoblotting. WT CHO cells, HSPG-deficient CHO cells, and L6 cells stably expressing FGFR1c together with β Klotho WT or β Klotho Δ RBA were grown in 100-mm plates to >80% confluence. The cells were stimulated with either FGF1 or FGF21 (at indicated concentrations) in the presence or absence of heparin (5 μ g/mL) for various time points (as indicated) at 37 $^{\circ}$ C, lysed, and incubated with the appropriate antibodies overnight at 4 $^{\circ}$ C. The immunoprecipitates were then washed and applied to sodium dodecyl-sulfate polyacrylamide gel electrophoresis (SDS-PAGE) followed by immunoblotting with various antibodies as indicated.

Calcium Imaging. WT CHO cells and HSPG-deficient cells stably expressing FGFR1c together with β Klotho were plated onto 35-mm glass-bottom dishes (MatTek) in phenol-red free DMEM (Gibco) supplemented with 10% FBS (Gibco) and grown to ~75% confluence the next day. The cells were starved in serum-free media for at least 2 h and then incubated with Calbryte 520 AM fluorescent calcium indicator (5 μ M, AAT Bioquest) for 30 min at 37 $^{\circ}$ C. The cells were washed three times and then imaged at 37 $^{\circ}$ C on a Nikon Eclipse Ti2 microscope using a 10 \times objective and a green fluorescent protein (GFP) excitation/emission filter set. Images were acquired every 5 s for 20 min with 200-ms exposure times. Ligands were added (at indicated concentrations) after 5 min of recording to obtain a baseline signal. Images were analyzed using ImageJ, and intensities of individual cells were calculated by taking the average intensity of a cell and subtracting the average intensity of a nearby region. Background-subtracted intensities during the last 10 baseline frames were averaged and used to normalize the change in fluorescence ($\Delta F/F_0$) upon ligand addition.

Single-Molecule TIRFM Imaging. WT CHO cells, HSPG-deficient CHO cells, and L6 cells were plated on 35-mm glass-bottom dishes (MatTek Corporation) and transfected with 0.25 μ g HaloTag β Klotho plasmid alone or together with 1 μ g FGFR1c plasmid the next day using Lipofectamine 3000 reagent (Invitrogen), according to the manufacturer's instructions. The cells were labeled with 0.25 μ M Alexa488 HaloTag ligand (Promega) for 15 min at 37 $^{\circ}$ C and then washed three times with phenol-red-free DMEM. The cells were immediately imaged at 37 $^{\circ}$ C and 5% CO₂ in a cage incubator (OkoLab) housing a Nikon Eclipse Ti2 microscope (Nikon) equipped with a motorized Ti-LA-HTIRF module with a 15-mW LU-N4 488 laser, using a CFI Plan Apochromat λ 100 \times /1.45 oil TIRF objective and a Prime95B complementary metal oxide semiconductor camera (Teledyne Photometrics). Images were acquired using a 100-ms exposure time at 10 Hz with the laser power set at 100%. The penetration depth of the evanescent field was ~118 nm. Particles were localized and tracked using the Matlab software GaussStorm (45, 46). Briefly, the particles were automatically detected by using a bandpass filter to remove noise, followed by convolution with a Gaussian kernel, and then the selection of the above-threshold pixels. The particles were then fitted with elliptical two-dimensional (2D) Gaussian functions, which yielded their intensities expressed as the volume under the curve. The particles were tracked frame to frame using a tracking algorithm with a tracking window of seven pixels between consecutive frames. The distribution of the displacements of single particles was used to calculate a mean diffusion coefficient in a field of view encompassing an entire cell.

Immunofluorescence. WT CHO cells stably expressing FGFR1c were plated onto 35-mm glass-bottom dishes (MatTek) and transfected with 1 μ g HaloTag- β Klotho WT or HaloTag- β Klotho Δ RBA plasmid the next day using Lipofectamine 3000 reagent (Invitrogen), according to the manufacturer's instructions. The cells were

labeled with 0.25 μ M Alexa488 HaloTag ligand (Promega) for 15 min at 37 $^{\circ}$ C, washed three times, and then stimulated with FGF1 (10 nM) for various time points (as indicated). After each time point, the cells were fixed in 4% paraformaldehyde for 15 min at room temperature, washed in PBS three times for 5 min, incubated for 1 h in blocking buffer (5% normal goat serum, 0.3% Triton X-100), and then incubated overnight at 4 $^{\circ}$ C with primary antibody against LAMP1 (Cell Signaling Technology). The cells were washed in PBS three times for 5 min, incubated for 1 h with Alexa568-conjugated goat anti-rabbit secondary antibody

(5% normal goat serum, 0.3% Triton X-100), and washed in PBS three times. Images were acquired with a Zeiss LSM 880 Airyscan confocal microscope.

Data, Materials, and Software Availability. All study data are included in the article and/or *SI Appendix*.

Author affiliations: ^aDepartment of Pharmacology, Yale University School of Medicine, New Haven, CT 06520

1. V. P. Eswarakumar, I. Lax, J. Schlessinger, Cellular signaling by fibroblast growth factor receptors. *Cytokine Growth Factor Rev.* **16**, 139–149 (2005).
2. N. Turner, R. Grose, Fibroblast growth factor signalling: From development to cancer. *Nat. Rev. Cancer* **10**, 116–129 (2010).
3. K. Dorey, E. Amaya, FGF signalling: Diverse roles during early vertebrate embryogenesis. *Development* **137**, 3731–3742 (2010).
4. M. Goldfarb, Fibroblast growth factor homologous factors: Evolution, structure, and function. *Cytokine Growth Factor Rev.* **16**, 215–220 (2005).
5. C. Wang, B. C. Chung, H. Yan, S.-Y. Lee, G. S. Pitt, Crystal structure of the ternary complex of a NaV C-terminal domain, a fibroblast growth factor homologous factor, and calmodulin. *Structure* **20**, 1167–1176 (2012).
6. M. Sochacka *et al.*, FHF1 is a bona fide fibroblast growth factor that activates cellular signaling in FGFR-dependent manner. *Cell Commun. Signal.* **18**, 69 (2020).
7. M. A. Lemmon, J. Schlessinger, Cell signaling by receptor tyrosine kinases. *Cell* **141**, 1117–1134 (2010).
8. D. M. Ornitz, N. Itoh, The fibroblast growth factor signaling pathway. *Wiley Interdiscip. Rev. Dev. Biol.* **4**, 215–266 (2015).
9. T. Spivak-Kroizman *et al.*, Heparin-induced oligomerization of FGF molecules is responsible for FGF receptor dimerization, activation, and cell proliferation. *Cell* **79**, 1015–1024 (1994).
10. S. K. Olsen *et al.*, Insights into the molecular basis for fibroblast growth factor receptor autoinhibition and ligand-binding promiscuity. *Proc. Natl. Acad. Sci. U.S.A.* **101**, 935–940 (2004).
11. S. Lee *et al.*, Structures of β -klotho reveal a 'zip code'-like mechanism for endocrine FGF signalling. *Nature* **553**, 501–505 (2018).
12. J. Schlessinger *et al.*, Crystal structure of a ternary FGF-FGFR-heparin complex reveals a dual role for heparin in FGFR binding and dimerization. *Mol. Cell* **6**, 743–750 (2000).
13. M. Mohammadi, S. K. Olsen, O. A. Ibrahim, Structural basis for fibroblast growth factor receptor activation. *Cytokine Growth Factor Rev.* **16**, 107–137 (2005).
14. R. Goetz *et al.*, Molecular insights into the klotho-dependent, endocrine mode of action of fibroblast growth factor 19 subfamily members. *Mol. Cell. Biol.* **27**, 3417–3428 (2007).
15. I. Urakawa *et al.*, Klotho converts canonical FGF receptor into a specific receptor for FGF23. *Nature* **444**, 770–774 (2006).
16. Y. Ogawa *et al.*, BetaKlotho is required for metabolic activity of fibroblast growth factor 21. *Proc. Natl. Acad. Sci. U.S.A.* **104**, 7432–7437 (2007).
17. H. Kurosu *et al.*, Regulation of fibroblast growth factor-23 signaling by klotho. *J. Biol. Chem.* **281**, 6120–6123 (2006).
18. A. Kharitonov *et al.*, FGF-21/FGF-21 receptor interaction and activation is determined by betaKlotho. *J. Cell. Physiol.* **215**, 1–7 (2008).
19. M. Kuro-O, The Klotho proteins in health and disease. *Nat. Rev. Nephrol.* **15**, 27–44 (2019).
20. R. Goetz *et al.*, Isolated C-terminal tail of FGF23 alleviates hypophosphatemia by inhibiting FGF23-FGFR-Klotho complex formation. *Proc. Natl. Acad. Sci. U.S.A.* **107**, 407–412 (2010).
21. G. Chen *et al.*, α -Klotho is a non-enzymatic molecular scaffold for FGF23 hormone signalling. *Nature* **553**, 461–466 (2018).
22. R. Kharitonov, DiMarchi, FGF21 revolutions: Recent advances illuminating FGF21 biology and medicinal properties. *Trends Endocrinol. Metab.* **26**, 608–617 (2015).
23. F. M. Fisher, E. Maratos-Flier, Understanding the physiology of FGF21. *Annu. Rev. Physiol.* **78**, 223–241 (2016).
24. L. D. BonDurant, M. J. Potthoff, Fibroblast growth factor 21: A versatile regulator of metabolic homeostasis. *Annu. Rev. Nutr.* **38**, 173–196 (2018).
25. S. A. Klierer, D. J. Mangelsdorf, A dozen years of discovery: Insights into the physiology and pharmacology of FGF21. *Cell Metab.* **29**, 246–253 (2019).
26. K. C. Coate *et al.*, FGF21 is an exocrine pancreas secretagogue. *Cell Metab.* **25**, 472–480 (2017).
27. Y. Suzuki *et al.*, FGF23 contains two distinct high-affinity binding sites enabling bivalent interactions with α -Klotho. *Proc. Natl. Acad. Sci. U.S.A.* **117**, 31800–31807 (2020).
28. K. Lidholt *et al.*, A single mutation affects both N-acetylglucosaminyltransferase and glucuronosyltransferase activities in a Chinese hamster ovary cell mutant defective in heparan sulfate biosynthesis. *Proc. Natl. Acad. Sci. U.S.A.* **89**, 2267–2271 (1992).
29. M. Roghani, D. Moscatelli, Basic fibroblast growth factor is internalized through both receptor-mediated and heparan sulfate-mediated mechanisms. *J. Biol. Chem.* **267**, 22156–22162 (1992).
30. S. Vainikka *et al.*, Signal transduction by fibroblast growth factor receptor-4 (FGFR-4). Comparison with FGFR-1. *J. Biol. Chem.* **269**, 18320–18326 (1994).
31. M. Asada *et al.*, Glycosaminoglycan affinity of the complete fibroblast growth factor family. *Biochim. Biophys. Acta* **1790**, 40–48 (2009).
32. M. Harada *et al.*, FGF9 monomer-dimer equilibrium regulates extracellular matrix affinity and tissue diffusion. *Nat. Genet.* **41**, 289–298 (2009).
33. X. Qu *et al.*, Glycosaminoglycan-dependent restriction of FGF diffusion is necessary for lacrimal gland development. *Development* **139**, 2730–2739 (2012).
34. A. K. Powell, D. G. Fernig, J. E. Turnbull, Fibroblast growth factor receptors 1 and 2 interact differently with heparin/heparan sulfate. Implications for dynamic assembly of a ternary signaling complex. *J. Biol. Chem.* **277**, 28554–28563 (2002).
35. R. Goetz *et al.*, Conversion of a paracrine fibroblast growth factor into an endocrine fibroblast growth factor. *J. Biol. Chem.* **287**, 29134–29146 (2012).
36. E. S. Kuzina *et al.*, Structures of ligand-occupied β -Klotho complexes reveal a molecular mechanism underlying endocrine FGF specificity and activity. *Proc. Natl. Acad. Sci. U.S.A.* **116**, 7819–7824 (2019).
37. Z. Huang *et al.*, Uncoupling the mitogenic and metabolic functions of FGF1 by tuning FGF1-FGF receptor dimer stability. *Cell Rep.* **20**, 1717–1728 (2017).
38. P. A. Dutchak *et al.*, Fibroblast growth factor-21 regulates PPAR γ activity and the antidiabetic actions of thiazolidinediones. *Cell* **148**, 556–67 (2012).
39. J. W. Jonker *et al.*, A PPAR γ -FGF1 axis is required for adaptive adipose remodelling and metabolic homeostasis. *Nature* **485**, 391–394 (2012).
40. S. Wang *et al.*, Adipocyte Piezo1 mediates obesogenic adipogenesis through the FGF1/FGFR1 signaling pathway in mice. *Nat. Commun.* **11**, 2303 (2020).
41. F. M. Fisher *et al.*, Obesity is a fibroblast growth factor 21 (FGF21)-resistant state. *Diabetes* **59**, 2781–2789 (2010).
42. C. Hale *et al.*, Lack of overt FGF21 resistance in two mouse models of obesity and insulin resistance. *Endocrinology* **153**, 69–80 (2012).
43. K. R. Markan *et al.*, FGF21 resistance is not mediated by downregulation of beta-klotho expression in white adipose tissue. *Mol. Metab.* **6**, 602–610 (2017).
44. J. H. Bae *et al.*, Asymmetric receptor contact is required for tyrosine autophosphorylation of fibroblast growth factor receptor in living cells. *Proc. Natl. Acad. Sci. U.S.A.* **107**, 2866–2871 (2010).
45. S. J. Holden *et al.*, Defining the limits of single-molecule FRET resolution in TIRF microscopy. *Biophys. J.* **99**, 3102–3111 (2010).
46. M. Fontana, C. Fijen, S. G. Lemay, K. Mathwig, J. Hohlbein, High-throughput, non-equilibrium studies of single biomolecules using glass-made nanofluidic devices. *Lab Chip* **19**, 79–86 (2018).